Linear muffin-tin-orbital and k · p calculations of effective masses and band structure of semiconducting diamond

M. Willatzen and M. Cardona
Max-Planck-Institut für Festkörperforschung,
Heisenbergstrasse 1, D-70569 Stuttgart, Federal Republic of Germany

N. E. Christensen
Institute of Physics and Astronomy, University of Aarhus, DK-8000 Aarhus C, Denmark
(Received 27 June 1994)

The electronic structure of semiconducting diamond is calculated by the scalar-relativistic linear muffin-tin-orbital method within the local-density approximation. Information about matrix elements, effective masses, and Luttinger parameters is extracted by comparison with $\mathbf{k}\cdot\mathbf{p}$ calculations. An extended 16×16 $\mathbf{k}\cdot\mathbf{p}$ calculation is performed using the parameters above as input so as to obtain the detailed band structure of the higher valence and lower conduction band states around the Γ point in the (110) direction.

I. INTRODUCTION

Semiconducting diamond is characterized by a number of interesting properties. The material has the highest thermal conductivity, the lowest dielectric constant, and the highest breakdown field and saturated electron velocity of all known semiconductors.[1] It has, therefore, the potential to become an important material for applications in semiconductor devices. Progress in the growth of single-crystal diamonds and thin films has recently resulted in a renewed interest in diamond.[2,3] In comparison with the diamondlike materials Ge and Si, our understanding of the electronic and optical properties of diamond is very poor, although considerable experimental and theoretical work has been performed over the past 40 years. This can be attributed to the difficulty in growing high-quality single crystals, the high energy gap of the material, the presence of strong impurity-induced absorption and, from the theoretical point of view, problems inherent in using the empirical pseudopotential method for atoms without p electrons in their cores.[4] Basic aspects, such as the values of carrier effective masses and the detailed band structure, are still unknown. Conduction band masses are difficult to obtain due to the absence of n-type semiconducting diamond. The valence band masses, or, equivalently, Luttinger parameters have been reported by a few authors[1,5–9] but the results are in disagreement with each other.

In the present work, we use scalar-relativistic band structure calculations in the local-density approximation assisted by $\mathbf{k}\cdot\mathbf{p}$ calculations to obtain information about momentum matrix elements, effective masses, and the Luttinger parameters of diamond. The parameters found in this way are subsequently used as input in a 16×16 $\mathbf{k}\cdot\mathbf{p}$ model[11] involving matrix elements between six $\Gamma_{25'}^{+v}$, six Γ_{15}^{-c}, two $\Gamma_{2'}^{-c}$, and two Γ_{1}^{+c} wave functions. This calculation allows us to determine the detailed upper valence and lower conduction band structures around the Γ point. Results along the (110) direction are presented.

II. LMTO BAND STRUCTURE CALCULATIONS

The electronic band structure of diamond is calculated here within the framework of density-functional theory (DFT) using the local-density approximation (LDA). This is done by means of the self-consistent scalar-relativistic LMTO method.[12] Each unit cell consists of four "atoms," including two empty spheres, i.e., atomic spheres with no net nuclear charge positioned in the empty tetrahedral sites in order to obtain a close-packed structure.[13] Calculations are performed within the atomic-sphere approximation including the so-called "combined correction term."[14] Wave functions in each atomic sphere (including empty spheres) are expressed in terms of s, p, and d partial waves and, treating the spin-orbit interaction as a perturbation to the scalar-relativistic Hamiltonian, we find a Hamiltonian matrix of dimension 72×72 (4 atoms $\times$ 9 partial waves $\times$ 2 spin states). It is well known that the DFT-LDA calculation yields quite reliable results for the valence band structure but understimates the bandgap for all usual semiconductors. This is a consequence of the fact that LDA energy values are not exact single-particle energies. To overcome this problem, quasiparticle corrections to the Hamiltonian must be added. A perturbative way to include quasiparticle corrections is given by the GW approximation.[15,16] This approach is computationally very expensive and will not be used here. However, it is also known that the LDA wave functions are already very close to those obtained using the GW approximation.[15] We therefore expect momentum matrix elements to be well described by the LMTO calculations in the LDA approximation.

This fact is used in the present paper in order to determine effective masses and Luttinger parameters of diamond at the Γ point by using the LMTO-calculated momentum matrix elements as input in $\mathbf{k}\cdot\mathbf{p}$ models. The effective masses calculated in this way, and corrected for the discrepancy between the experimental and calculated energy gaps, are expected to be quite accurate since momentum matrix elements from LMTO calculations are supposed to be accurate. Our results are compared with the few data for diamond available in the literature. We also estimate the transverse and longitudinal effective masses at the conduction band minima located close to the X point. Finally, we determine the upper valence and lower conduction band structures of diamond as calculated from a 16×16 $\mathbf{k}\cdot\mathbf{p}$ model[11] using the parameters found above. In this manner the question of the possible existence of valence band maxima away from $\mathbf{k}$ is negatively answered.

III. k · p THEORY

In diamond, where spin-orbit effects are very small,[5,8] we use the following expressions for effective masses at the Γ point given by Kane[17] and Shtivel'man[18] ($\Delta_0 = 0$):

(100) direction :

$$\begin{aligned} m_1^{-1} &= 1 + 2L \ , \\ m_2^{-1} &= m_3^{-1} = 1 + 2M \ ; \end{aligned} \tag{1}$$

(111) direction:

$$\begin{aligned} m_1^{-1} &= 1 + \frac{2L + 4M + 4N}{3} \ , \\ m_2^{-1} &= m_3^{-1} = 1 + \frac{4M + 2L - 2N}{3} \ ; \end{aligned} \tag{2}$$

(110) direction:

$$\begin{aligned} m_1^{-1} &= 1 + L + M + N \ , \\ m_2^{-1} &= 1 + 2M + \frac{1}{2}(L - M - N) - \frac{1}{2} \mid L - M - N \mid \ , \\ m_3^{-1} &= 1 + 2M + \frac{1}{2}(L - M - N) + \frac{1}{2} \mid L - M - N \mid \ . \end{aligned} \tag{3}$$

Here, m_2 (m_3) is the light-hole (heavy-hole) mass, and m_1 is usually referred to as the split-off band effective mass in the case of nonvanishing spin-orbit interaction. For the s-type conduction band ($\Gamma_{2'}^{-c}$) the effective mass is isotropic and given by

$$m_4^{-1} = 1 + 2A' + \frac{2P^2}{E_{\Gamma_{2'}^{-c}} - E_{\Gamma_{25'}^{+v}}} \ . \tag{4}$$

Note that the s-type conduction band ($\Gamma_{2'}^{-c}$) in diamond is located at a higher energy than the p-type conduction band (Γ_{15}^{-c}), see Fig. 1. In our discussion of the effective masses and momentum matrix elements, we use atomic units, i.e., $m_0 = e = \hbar = 1$, energies in Hartree units, and Luttinger parameters in units of $\hbar^2/2m_0$.

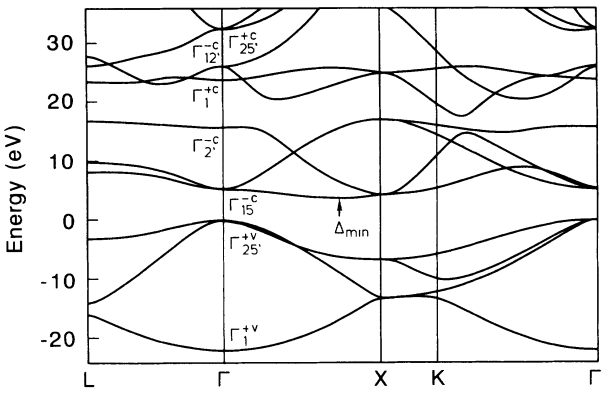

FIG. 1. Band structure of diamond as calculated from the LMTO method in the local-density approximation.

The parameters L, M, N, and A' are given by Dresselhaus, Kip, and Kittel[19] and Kane:[17]

$$\begin{aligned} L &= F + 2G \ , \\ M &= H_1 + H_2 \ , \\ N &= F - G + H_1 - H_2 \ , \end{aligned} \tag{5}$$

where

$$\begin{aligned} F &= -\sum_j{}' \frac{|\langle X \mid p_x \mid u_j \rangle|^2}{E_j - E_{\Gamma_{25'}^{+}}} - \frac{P^2}{E_{\Gamma_{2'}^{-}} - E_{\Gamma_{25'}^{+}}} \\ &\simeq -\frac{P^2}{E_{\Gamma_{2'}^{-}} - E_{\Gamma_{25'}^{+}}} \ , \\ G &= -\frac{1}{2}\sum_j{}^{\Gamma_{12'}^{-}} \frac{|\langle X \mid p_x \mid u_j \rangle|^2}{E_j - E_{\Gamma_{25'}^{+}}} = -\frac{R^2}{E_{\Gamma_{12'}^{-}} - E_{\Gamma_{25'}^{+}}} \ , \\ H_1 &= -\sum_j{}^{\Gamma_{15}^{-}} \frac{|\langle X \mid p_y \mid u_j \rangle|^2}{E_j - E_{\Gamma_{25'}^{+}}} = -\frac{Q^2}{E_{\Gamma_{15'}^{-}} - E_{\Gamma_{25'}^{+}}} \ , \\ H_2 &= -\sum_j{}^{\Gamma_{25}^{-}} \frac{|\langle X \mid p_y \mid u_j \rangle|^2}{E_j - E_{\Gamma_{25'}^{+}}} \simeq 0 \ , \\ A' &= \sum_j{}'^{\Gamma_{25'}^{+}} \frac{|\langle S \mid p_x \mid u_j \rangle|^2}{E_{\Gamma_{2'}^{-}} - E_j} \ , \end{aligned} \tag{6}$$

and

$$\begin{aligned} P &= i\left\langle \Gamma_{25',x}^{+v} \mid p_x \mid \Gamma_{2'}^{-c} \right\rangle \ , \\ Q &= i\left\langle \Gamma_{25',x}^{+v} \mid p_y \mid \Gamma_{15,z}^{-c} \right\rangle \ , \\ R &= i\left\langle \Gamma_{25',x}^{+v} \mid p_x \mid \Gamma_{12',1}^{-} \right\rangle \ . \end{aligned} \tag{7}$$

The $\Gamma_{12',1}^{-}$ state in Eq. (7) is equivalent to the γ_1^- state of the representation $\Gamma_{12'}^{-}$ in Dresselhaus's notation.[19] In

Eq. (6), primes on the summation symbols mean that the $\Gamma_{2'}^{-}$ conduction band states (for F) and the $\Gamma_{25'}^{+}$ valence band states (for A') are not to be summed over. Note that the coefficient $\frac{1}{2}$ in the expression for G comes from Dresselhaus's definition of G,[19] where summation is over one of the two states representing $\Gamma_{12'}^{-}$. Our expression agrees, therefore, with Dresselhaus's. The first term in F and H_2 vanishes in our approach, since we neglect coupling to the high-energy f-like bands. We expect A' to give important contributions to the conduction band mass m_4 in (4), since the $\Gamma_{2'}^{-}$ and $\Gamma_{25'}^{+}$ conduction bands are relatively close in energy, see Fig. 1 (the energy separation $E_{\Gamma_{25'}^{+c}} - E_{\Gamma_{2'}^{-}}$ is close to the energy difference $E_{\Gamma_{2'}^{-c}} - E_{\Gamma_{25'}^{+v}}$).

In the calculation of Luttinger parameters γ_1, γ_2, γ_3, and κ we use the following expressions:

$$\begin{aligned}\gamma_1 &= -\frac{1}{3}(2F + 4G + 4M) - 1 ,\\ \gamma_2 &= -\frac{1}{6}(2F + 4G - 2M) ,\\ \gamma_3 &= -\frac{1}{6}(2F - 2G + 2M) ,\\ \kappa &= -\frac{1}{3}\gamma_1 + \frac{2}{3}\gamma_2 + \gamma_3 - \frac{2}{3} .\end{aligned} \tag{8}$$

Following the determination of the matrix elements P, Q, and A' from the LMTO results, and using the parameters $P''' = i\langle\Gamma_{15,x}^{-c} \mid p_x \mid \Gamma_1^{+c}\rangle = 0.7480$ a.u. (LMTO), $E_0''' = E_{\Gamma_6^{+c}}(\text{upper}) - E_{\Gamma_8^{+v}} = 24.0$ eV (LMTO), $\Delta_0 = E_{\Gamma_8^{+v}} - E_{\Gamma_7^{+v}} = 0.013$ eV (LMTO), and $\Delta_0' = E_{\Gamma_8^{-c}} - E_{\Gamma_7^{-c}} = 0.012$ eV (LMTO), we are in a position to perform a more accurate calculation based on a 16×16 $\mathbf{k}\cdot\mathbf{p}$ Hamiltonian matrix[11] involving matrix elements between six $\Gamma_{25'}^{+v}$, six Γ_{15}^{-c}, two $\Gamma_{2'}^{-c}$, and two Γ_1^{+c} wave functions. As a basis we take the linear combinations of these wave functions which correspond to $(\frac{1}{2},\pm\frac{1}{2})$, $(\frac{3}{2},\pm\frac{3}{2})$, and $(\frac{3}{2},\pm\frac{1}{2})$ angular-momentum states with z (i.e., [001]) as the quantization axis. Portions of the Hamiltonian are given in Table 1 of Ref. 10 (between the Γ_7^{-c}, Γ_8^{-c}, and Γ_7^{+v}, Γ_8^{+v}, Γ_6^{+} states) and in the appendix of Ref. 11 (the "diagonal" matrix connecting the $\Gamma_{25'}^{+v}$ states with themselves).

We recall that for diamond-type materials with inversion symmetry, the parameters:[11] $\Delta^{-} = \frac{3}{2}i\langle(\frac{1}{2}\frac{1}{2}_v) \mid H_{\text{s.o.}} \mid (\frac{1}{2}\frac{1}{2}_c)\rangle$, $P' = i\langle\Gamma_{15,x}^{-c} \mid p_x \mid \Gamma_{2'}^{-c}\rangle$, C_k and C_k' (coefficients of the linear k terms in the Hamiltonian produced mainly by bilinear second-order perturbation terms in $H_{\mathbf{k}\cdot\mathbf{p}}$ and $H_{\text{s.o.}}$ for the Γ_8^{+v} and Γ_8^{-c} bands, respectively) which are important in zincblende-type semiconductors *all vanish*. Here, $H_{\mathbf{k}\cdot\mathbf{p}}$ is the $\mathbf{k}\cdot\mathbf{p}$ part of the Hamiltonian, and $H_{\text{s.o.}}$ is the spin-orbit contribution.

IV. NUMERICAL RESULTS

The band structure of diamond calculated within the local-density approximation using the self-consistent scalar-relativistic LMTO method is shown in Fig. 1. We emphasize that the adjusting potential method first described by Christensen[20] using δ-like potentials centered at the atoms to shift the s-like states, and later extended to include potentials shifting the p-like states,[21] cannot be used to adjust the LMTO gaps of diamond. The lowest direct gap involving the p-like conduction band states at the Γ point is underestimated in our calculation by $\sim$ 2.0 eV compared to the experimental direct band gap of 7.3 eV. Unfortunately, we have not found a way to add adjusting potentials to the self-consistent LMTO band structure calculation so as to shift the p states by about 2.0 eV. Therefore, we apply here the LMTO band structure calculations in the local-density approximation to obtain the momentum matrix elements necessary for the evaluation of effective masses. As mentioned earlier, we expect these matrix elements to be quite well described by the LDA, since wave functions are close to those found in GW calculations.

TABLE I. Energies in eV at the Γ point and the X point of diamond, and the indirect energy gap.

	LMTO (LDA)	GW, Hybertsen and Louie (Ref. 15)	Pseudopotential Bachelet *et al.* (Ref. 22)	Expt. (Ref. 23)
$E_{\Gamma_1^{+v}}$	−21.90	−23.0	−21.45	−24.2 ± 1, −21 ± 1
$E_{\Gamma_{25'}^{+v}}$	0.0	0.0	0.0	0.0
$E_{\Gamma_{15}^{-c}}$	5.36	7.5	5.40	7.3
$E_{\Gamma_{2'}^{-c}}$	15.88	14.8	13.38	15.3 ± 0.5
$E_{\Gamma_1^{+c}}$	24.00			
$E_{\Gamma_{12'}^{-c}}$	26.33			
$E_{\Gamma_{25'}^{+c}}$	32.49			
$E_{X_1^v}$	−13.16		−12.65	
$E_{X_4^v}$	−6.66		−6.22	
$E_{X_1^c}$	4.36		4.63	
$E_{X_4^c}$	17.13		16.73	
Δ_0	0.013			0.006
Δ_0'	0.012			
$E_{\text{gap}}^{\text{ind}}$	3.74	5.6		5.48

In Table I we show the calculated energies at the Γ point and the X point for diamond using the LMTO method in the local-density approximation. This table also contains the theoretical results of Hybertsen and Louie[15] (GW), Bachelet *et al.*,[22] (pseudopotential), and the experimental data.

The finer structure around $k = 0$ has been studied by dividing the [100], [110], and [111] directions of the Brillouin zone into a dense **k** mesh. By fitting a straight line to the calculated electronic energies versus k^2 in the immediate vicinity of point Γ, the slopes yield the LDA effective masses for the different directions. The effective mass of the s-like conduction band $\Gamma_{2'}^{-c}$, m_4, is found to be isotropic, in contrast to the split-off, heavy-hole, and light-hole masses, which show a strong anisotropy described by Dresselhaus's parameters L, M, N, or equivalently, the Luttinger parameters γ_1, γ_2, and γ_3.

In Table II we list the LDA effective masses calculated by the LMTO method and the experimentally corrected effective masses obtained from our LMTO and **k** · **p** calculations. We have listed both the masses for $\Delta_0 = 0$ obtained directly from our calculations and those near Γ for $\Delta_0 \neq 0$ ($m_{\rm hh}$, $m_{\rm lh}$, $m_{\rm s.o.}$) calculated with the expressions given in Eqs. (46) and (47) of Ref. 17. The experimentally corrected effective mass values given in Table II were calculated using the following scheme: First, we determine the matrix elements P^2, Q^2, and R^2 in (6) using the energies in Table I and the effective masses in Table II calculated with the LMTO method in the local-density approximation. These matrix elements are solely determined by the wave functions and, therefore, they are expected to be well described by the LDA approximation. From P^2, Q^2, and R^2, and the experimental energy values in Table I, we obtain the renormalized (or corrected) effective masses in the second column of Table II. In Table III we give the matrix elements and parameters obtained from the LMTO and **k** · **p** calculations.

TABLE II. Effective masses of the p-like valence band states and lower s-like conduction band state (m_4) of diamond calculated in the present work. $m_\perp$ is the calculated effective mass at the conduction band minimum located in the Brillouin zone at $\frac{2\pi}{a}(0.742, 0, 0)$. m_1, m_2, and m_3 represent the hole masses in the absence of spin-orbit splitting while $m_{\rm hh}$, $m_{\rm lh}$, and $m_{\rm so}$ represent the physically more meaningful hole masses including the spin-orbit splitting at Γ. The LMTO-corrected effective masses in the third column are calculated from the LDA effective masses in the second column corrected for the discrepancy between the experimental and calculated energy gaps.

	LMTO (LDA)	LMTO corr.
m_1^{100}	0.482	0.466
m_1^{111}	0.147	0.198
m_1^{110}	0.178	0.232
m_2^{100}	0.244	0.366
m_2^{111}	0.575	0.778
m_2^{110}	0.243	0.366
m_3^{100}	0.244	0.366
m_3^{111}	0.575	0.778
m_3^{110}	1.808	1.783
m_4	2.375	2.030
$m_\perp$	0.258	0.341
$m_{\rm so}$	0.292	0.394
$m_{\rm hh}^{100}$	0.364	0.427
$m_{\rm hh}^{111}$	0.575	0.778
$m_{\rm hh}^{110}$	0.519	0.690
$m_{\rm lh}^{100}$	0.244	0.366
$m_{\rm lh}^{111}$	0.196	0.264
$m_{\rm lh}^{110}$	0.203	0.276

TABLE III. Matrix elements (in atomic units) and other band parameters at Γ obtained by the LMTO and **k** · **p** calculations. If we assume that A' is due exclusively to the interaction of $\Gamma_{2'}^{-c}$ with $\Gamma_{25'}^{+c}$ we obtain for the corresponding matrix element $P'' = 0$.

F	−0.5325
M	−1.868
G	−0.520
P	0.538
Q	0.708
R	0.709
A'''	−0.786
P'''	0.7480

In Table IV we list the corrected Luttinger parameters. These can also be derived from the corrected effective masses given in Table II. Also shown are all the values for the Luttinger parameters reported to date. As can be seen, there are considerable discrepancies among the results. The values of Bashenov, Gontar, and Petukhov[6] and Lawaetz,[5] however, agree quite well with our data.

In Fig. 2 we show the upper valence band structure and lower conduction band structure at the Γ point in the (110) direction calculated with the 16 × 16 **k** · **p** Hamiltonian using the experimental direct gap values. Furthermore, we obtain from the 16 × 16 **k** · **p** Hamiltonian band structure analysis values for the Γ_{15}^{-c} p-like

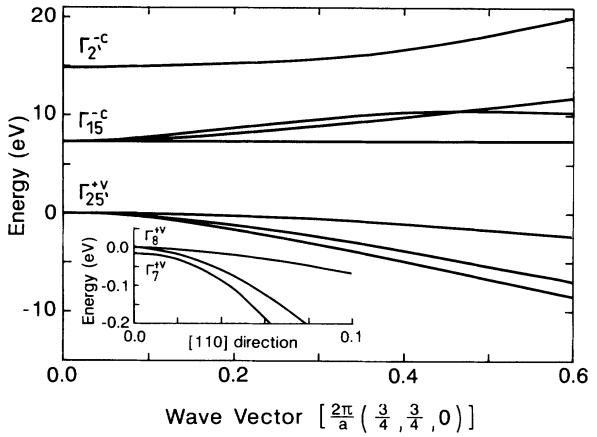

FIG. 2. The upper valence and lower conduction band structures of diamond as calculated from the 16× 16 **k** · **p** model in the (110) direction. 0 (1) on the x axis corresponds to the Γ point (K point). The zero of energy has been chosen at the Γ_8^{+v} state. The inset shows the detailed band structure of the upper valence band close to the Γ point.

TABLE IV. Luttinger parameters for diamond.

	γ_1	γ_2	γ_3	κ
Present work	2.54	−0.10	0.63	−0.95
Lawaetz[a]	4.62	−0.38	1.00	−1.46
Eremets[b]	4.24	0.82	1.71	0.18
Bashenov[c]	2.19	−0.12	0.87	−0.61
Bagguley[d]	2.16	−0.23	−0.15	−1.69
Rauch[e]	0.94	0.22	0.25	−0.58
Kono[f]	0.67, 0.67	−0.57, −0.98	−2.23, 0.56	−3.50, −0.98

[a]Reference 5.
[b]Reference 1.
[c]Reference 6.
[d]Reference 7.
[e]Reference 8.
[f]Reference 9.

conduction band effective masses:

$$m_1^{c110} = 0.340 ,$$
$$m_2^{c110} = 1.252 ,$$
$$m_3^{c110} = 0.5335 . \quad (9)$$

These values can, of course, be obtained directly from a $\mathbf{k}\cdot\mathbf{p}$ analysis similar to that presented above in the s-like conduction and p-like valence band states. The most important conclusion from Fig. 2 is that the valence band maximum occurs at Γ, contrary to a suggestion in Ref. 9.

We found the conduction band minimum to be located at $\frac{2\pi}{a}(0.742, 0, 0)$, i.e., close to the X point of the Brillouin zone, see Fig. 1. Our LMTO calculations give the following values for the lower conduction band effective masses at the conduction band minimum and the indirect band gap in eV [$m_\parallel$ is the effective mass in the (100) direction and $m_\perp$ is the effective mass in the (010) direction]:

$$m_\parallel^{\mathrm{LDA}} = 1.50 ,$$
$$m_\perp^{\mathrm{LDA}} = 0.26 ,$$
$$E_{\mathrm{gap}}(\mathrm{indirect}) = 3.74 . \quad (10)$$

In analogy with the previous prescription, we correct these masses for the difference between the LDA value of the indirect gap (3.74 eV) and the experimental one (5.48 eV). This difference reflects itself in a difference by the same amount, i.e., 1.74 eV, between the direct gap at Δ_{min} which determines the mass at Δ_{min}. In this manner we obtain the corrected value of $m_\perp = 0.341$. Such corrections should alter little the value of $m_\parallel$ which is determined by much larger gaps.

V. CONCLUSIONS

In summary, we have performed self-consistent scalar-relativistic LMTO band-structure calculations of diamond in the local-density approximation. From the wave functions, matrix elements for the $\mathbf{k}\cdot\mathbf{p}$ Hamiltonian are determined which are expected to be accurate although obtained with the LDA approximation: quasiparticle corrections to the Hamiltonian leave the wave functions more or less unaffected. The matrix elements so obtained and the experimental energy gap values allow us to calculate renormalized effective masses and Luttinger parameters for diamond, parameters which are still under debate for this material. Following the determination of renormalized parameters, we perform a 16×16 $\mathbf{k}\cdot\mathbf{p}$ Hamiltonian analysis in order to obtain the detailed band structure of the upper valence and lower conduction band states around the Γ point in the (110) direction and to settle the question of the possible existence of valence band maxima away from Γ. Our calculations show that the valence band maximum is located at the Γ point.

ACKNOWLEDGEMENT

M.W. acknowledges financial support from the Danish National Science Research Council (Contract 11-0855-1).

[1] M. I. Eremets, Semicond. Sci. Technol. **6**, 439 (1991).
[2] T. R. Anthony, W. F. Banholzer, J. F. Fleischer, Lanhua Wei, P. K. Kuo, R. L. Thomas, and R. W. Pryor, Phys. Rev. B **42**, 1104 (1990).
[3] *Thin Film Diamond*, Royal Society Book, edited by A. Lettington and J. W. Steeds (Chapman and Hall, London, 1994).
[4] M. Cardona and N. E. Christensen, Solid State Commun. **58**, 421 (1986).
[5] P. Lawaetz, Phys. Rev. B **4**, 3460 (1971).
[6] V. K. Bashenov, A. G. Gontar, and A. G. Petukhov, Phys. Status Solidi B **108**, K139 (1981).
[7] D. M. S. Bagguley, G. Vella-Coleiro, S. D. Smith, and C. J. Summers, J. Phys. Soc. Jpn. **21** (Suppl.), 244 (1966).
[8] C. J. Rauch, in *Proceedings of the International Conference on the Physics of Semiconductors, Exeter, 1962*, edited by A. C. Stickland (The Institute of Physics and the Physical Society, London, 1962), p. 276.
[9] J. Kono, S. Takeyama, T. Takamasu, N. Miura, N. Fujimori, Y. Nishibayashi, T. Nakajima, and K. Tsuji, Phys. Rev. B **48**, 10 917 (1993).
[10] U. Rössler, Solid State Commun. **49**, 943 (1984).
[11] M. Cardona, N. E. Christensen, and G. Fasol, Phys. Rev. B **38**, 1806 (1988).
[12] O. K. Andersen, Phys. Rev. B **12**, 3060 (1975).
[13] D. Glötzel, B. Segal, and O. K. Andersen, Solid State Com-

mun. **36**, 403 (1980).
[14] G. B. Bachelet and N. E. Christensen, Phys. Rev. B **31**, 879 (1985).
[15] M. S. Hybertsen and S. G. Louie, Phys. Rev. B **34**, 5390 (1986).
[16] M. Rohlfing, P. Krüger, and J. Pollmann, Phys. Rev. B **24**, 17 791 (1993).
[17] E. O. Kane, in *Semiconductors and Semimetals*, edited by R. K. Willardson and A. C. Beer (Academic, New York, 1966), Vol. 1, p. 75. Note that the expressions of F, G, and H_1 found in the literature differ sometimes from those given here and in the present work by a factor of 2.
[18] K. Ya. Shtivel'man, Fiz. Tverd. Tela (Leningrad) **5**, 348 (1963)[Sov. Phys. Solid State **5**, 252 (1963)].
[19] G. Dresselhaus, A. F. Kip, and C. Kittel, Phys. Rev. **98**, 368 (1955).
[20] N. E. Christensen, Phys. Rev. B **30**, 5753 (1984).
[21] T. Brudevoll, D. S. Citrin, M. Cardona, and N. E. Christensen, Phys. Rev. B **48**, 8629 (1993).
[22] G. B. Bachelet, H. S. Greenside, G. A. Baraff, and M. Schlüter, Phys. Rev. B **24**, 4745 (1981).
[23] *Numerical Data and Functional Relationships in Science and Technology*, edited by K. H. Hellwege and O. Madelung, Landolt-Börnstein, New Series, Group III, Vol. 22, Pt. a (Springer, Berlin, 1982).